Relative pollen productivity estimates of savanna taxa from southern Africa and their application to reconstruct shrub encroachment during the last century

Ximena Tabares,[1,2] iD **Gregor Ratzmann,[3] Stefan Kruse,[1] Martin Theuerkauf,[4] Benjamin Mapani[5] and Ulrike Herzschuh[1,2,6]**

Abstract

To understand the resilience of African savannas to global change, quantitative information on the long-term dynamics of vegetation is required. Past dynamics can be reconstructed with the REVEALS model, which requires pollen productivity estimates (PPE) that are calibrated using surface pollen and vegetation data. Here we calculated PPE values for five savanna taxa using the extended R-value (ERV) model and two pollen dispersal options: the Gaussian plume model (GPM) and the Lagrangian stochastic model (LSM). The ERV calculations failed to produce a reliable PPE for Poaceae. We therefore used Combretaceae as the reference taxon – although values obtained with Poaceae as the reference taxon are presented in the supplement. Our results indicate that Combretaceae is the taxon with the highest pollen productivity and *Grewia* the taxon with the lowest productivity. *Acacia* and *Dichrostachy*s are intermediate pollen producers. We find no clear indication of whether the GPM PPEs or the LSM PPEs are more realistic, but the differences between these values confirmed that the pollen fall speed has a greater effect in the modelling of GPM than in the LSM. We also applied REVEALS to the pollen record of Lake Otjikoto (northern Namibia) and obtained the first quantitative reconstruction of the last 130 years of vegetation history in the region. Cover estimates for Poaceae indicate the predominance of a semi-open landscape throughout the 20th century, while cover values below 50% since the 21st century correspond to a thick savanna. This change in grass cover is associated with the spread of *Vachellia, Senegalia* and *Grewia* reflecting an encroached state.

Introduction

Quantitative information on long-term vegetation dynamics in southern African savannas is necessary to characterize shrub encroachment (Hoffman et al., 2019; Stevens et al., 2016). Several studies have used compositional changes of fossil pollen records (Miller and Gosling, 2014; Neumann et al., 2010) or woodland/grassland pollen taxa ratios (Gil-Romera et al., 2010; Gillson, 2004) to track vegetation change in savannas qualitatively or semi-quantitatively. Quantitative reconstructions of past vegetation cover based on fossil pollen records remain a challenge due to the non-linearity of pollen-vegetation relationships (Prentice and Webb, 1986). Although some calibration efforts have been made using modern pollen analogues of savanna taxa (Duffin and Bunting, 2008; Julier et al., 2018; Schüler et al., 2014), calibrated fossil pollen records from southern African savannas are still lacking, even though such gained knowledge may have implications for land management.

Pollen deposition in the savanna is characterized by over-representation of wind-pollinated grasses and under-representation of the insect-pollinated shrubs and trees that dominate the vegetation (Duffin and Bunting, 2008; Mariani et al., 2016). Furthermore, it is known that assumptions on dispersal and productivity of the individual taxa eventually impact the reconstructed vegetation composition (Prentice, 1985). Whether and how such effects

also apply for savanna taxa in southern Africa, is currently unknown. Duffin and Bunting (2008) applied the extended R-value model (ERV; Parsons and Prentice, 1981) to calculate relative pollen productivity estimates (PPEs; Sugita, 1994) of savanna taxa by using the Prentice-Sugita model for pollen dispersal (Prentice, 1985, 1988; Sugita, 1993). This model is based on Sutton's equations of small particle dispersal and deposition (Sutton, 1947), which is a particular form of the Gaussian plume model (GPM; Jackson and Lyford, 1999). However, studies about

[1]Alfred Wegener Institute, Helmholtz Centre for Polar and Marine Research, Potsdam, Germany
[2]Institute of Biochemistry and Biology, Potsdam University, Potsdam, Germany
[3]Institute of Biology, Freie Universität Berlin, Berlin, Germany
[4]Institute of Botany and Landscape Ecology, Greifswald University, Greifswald, Germany
[5]Department of Geology, University of Namibia, Windhoek, Namibia
[6]Institute of Environmental Science and Geography, Potsdam University, Potsdam, Germany

Corresponding author:
Ximena Tabares, Institute of Biochemistry and Biology, Potsdam University, Am Mühlenberg 3, Potsdam 14476, Germany.
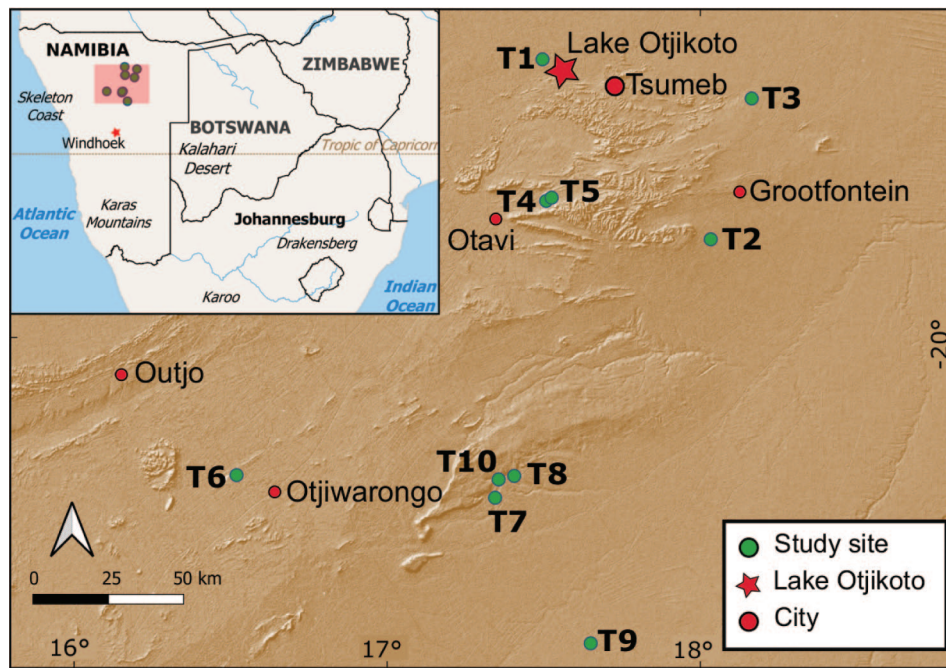Email: xtabares@uni-potsdam.de

Figure 1. Map of the study sites (created using Natural Earth data in QGIS).

Table 1. Overview of the study sites including GPS coordinates of the sample point in each transect. Mean annual precipitation (MAP) was estimated from climate cell gridded data (CRU TS v. 4.03; Harris et al., 2014), vegetation structure and landscape according to Mendelsohn et al. (2010).

Site_ID	Latitude	Longitude	Elevation (m)	MAP (mm)	Landscape	Vegetation structure
T1	−19.16366	17.4961	1212	406	Karstveld	Mixed woodland, broad-leaved taxa
T2	−19.70513	18.03364	1426	397	Karstveld	Mixed woodland, broad-leaved taxa
T3	−19.28155	18.16444	1297	425	Karstveld	Mixed woodland, broad-leaved taxa
T4	−19.58974	17.508012	1508	460	Karstveld	Mixed woodland, broad-leaved taxa
T5	−19.57997	17.52529	1513	460	Karstveld	Mixed woodland, broad-leaved taxa
T6	−20.41182	16.51911	1382	378	Thornbush savanna	Mixed woodland
T7	−20.47968	17.34482	1403	342	Thornbush savanna	Mixed woodland
T8	−20.41427	17.40593	1398	342	Thornbush savanna	Mixed woodland
T9	−20.91421	17.65009	1341	306	Central Kalahari	Acacia shrubland
T10	−20.42483	17.35616	1438	342	Thornbush savanna	Mixed woodland

dispersal of insect-pollinated taxa (Mariani et al., 2016) argue that mechanistic dispersal models, such as the Lagrangian stochastic model (LSM; Kuparinen et al., 2007) better display transport, particularly of large pollen grains, whose contribution is assumed to be anisotropic and to take place under unstable atmospheric conditions (Pérez et al., 2018). To date, the LSM has not been tested for modelling pollen dispersal of southern African savanna taxa.

In this study, we aim (1) to calculate fall-speed values and PPEs of the five main taxa of savanna vegetation in northern Namibia, and (2) to reconstruct past vegetation cover based on PPEs and fossil pollen data from Lake Otjikoto in north-central Namibia. Here we apply, for the first time in southern Africa, the LSM dispersal model (Kuparinen et al., 2007) to calculate PPEs and the REVEALS (Regional Estimates of Vegetation Abundance from Large Sites; Sugita, 2007; Theuerkauf et al., 2016) model to quantify landscape cover changes in semi-arid savanna environments.

Methods

Study sites

We investigated 10 sites in north-central Namibia (Figure 1). The distance between sites is at least 2 km to avoid spatial autocorrelation (Bunting et al., 2013) and the distance between the northernmost and the southernmost sites is approx. 200 km. The mean

annual rainfall in the study area ranges from 306 to 460 mm falling mainly in the summer months (October–March; Harris et al., 2014; Table 1).

The five northern sites (T1-T5) are located in Karstveld. This landscape is characterized by dominance of soluble dolomite and limestone in the substrate; cambisols and chromic luvisols are the main top soils (Mendelsohn et al., 2000). The vegetation consists of mixed woodland dominated by broadleaved taxa such as *Colophospermum mopane* (Benth.) Leonard, *Combretum imberbe* Wawra, *Combretum apiculatum* Sond. and *Terminalia prunioides* M.A. Lawson (Mendelsohn et al., 2000).

The sites T6 to T10 are found in the thornbush shrubland, except for the southernmost site (T9), which is in the central Kalahari. The local substrate at the southern sites consist of Kalahari sands and sands of the Etjo formation. The main top soils are ferralic and clay rich arenosols (Mendelsohn et al., 2010). Common vegetation types are mixed woodland and *Acacia* shrubland, which are characterized by *Terminalia sericea* Burch. ex DC., *Burkea africana* Hook., *Baikiaea plurijuga* Harms, *Vachellia erioloba* (E. Mey.) P.J.H. Hurter and *Senegalia mellifera* (Benth.) Seigler & Ebinger (Mendelsohn et al., 2010).

All study sites are situated on farms and used for cattle herding and reflect the main vegetation composition of their corresponding landscape (Table 1). Dominant encroacher species are *T.*
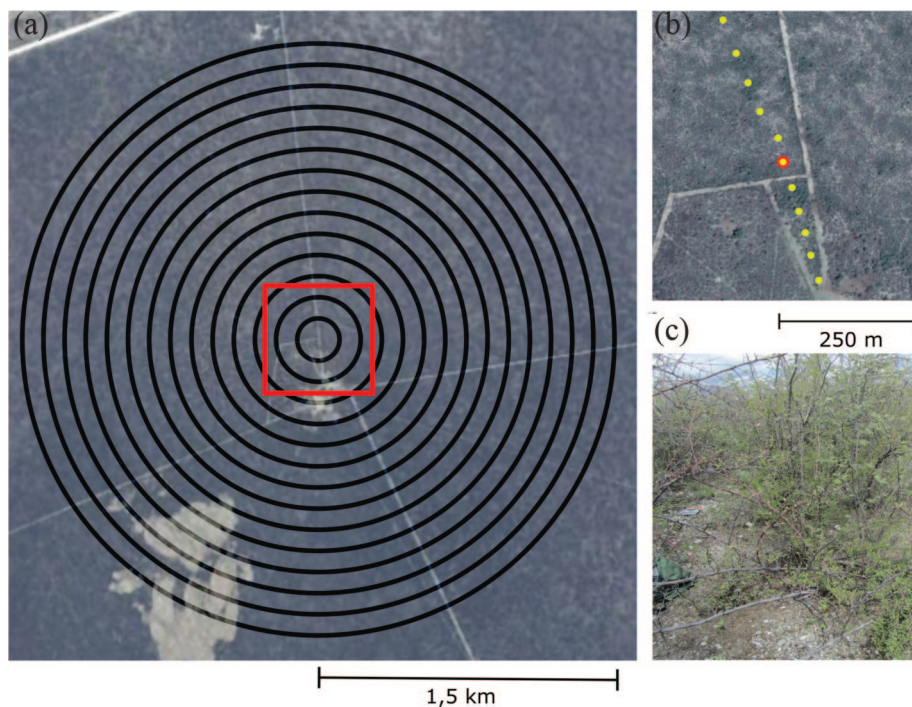
Figure 2. Vegetation sampling design. (a) Area of vegetation classified with satellite images using concentric rings. The red frame indicates the area surveyed on the field. (b) Vegetation plots along a transect in the field, where the central plot (red) is the sampling point. (c) Vegetation in the plot at site T1 (image by X. Tabares).

prunioides and *Dichrostachys cinerea* (L.) Wight & Arn. in the Karstveld, and *S. mellifera* in the thornbush sites (De Klerk, 2004).

Vegetation data

Vegetation composition was analysed within 7 km² for each study site using plot relevés as well as satellite imagery (Figure 2a). The relevés were used to identify plant species composition within a radius of 250 m from a pollen sampling point, while satellite imagery was used to map the spatial pattern of major vegetation types within a radius of 1.5 km.

Eleven relevés of 5 × 5 m were recorded during field work at each study site. The plots were spaced 50 m apart along a 500 m long transect (Figure 2b). Transects were defined according to the homogeneity of the vegetation and avoiding the presence of buildings in the studied area.

The plot located in the middle of the transect at each study site was chosen to take pollen samples (Figure 2b). For each of the central plots, surface soil samples (approx. 60 g) were collected from six subplots and pooled for subsequent pollen analysis.

Plant abundances in each plot were estimated using the Braun-Blanquet method (1964). We assigned scores to infer the relative percentage of plant cover in the ground and tree layers as described in Tabares et al. (2018).

At each study site, the relevés data from the corresponding 11 plots were combined into average cover values for each taxon. To match the pollen types Combretaceae, *Acacia, Grewia* and Poaceae, we merged the average cover of the corresponding *Senegalia* and *Vachellia* species under the *Acacia* type and *Grewia* species at the genus level, while grass cover and cover of Combretaceae taxa were aggregated at the family level.

Satellite imagery was used to estimate plant abundances within a radius of 1.5 km at each study site (satellite images courtesy of the DigitalGlobe Foundation: www.digitalglobefoundation.org). We used multispectral GeoEye-1 and WorldView-2 satellite images at 0.4 m resolution. All scenes were pan-sharpened and ortho-corrected. For each scene, training samples were manually

defined for three land-cover classes (bare soil, woody vegetation, grasses). The training samples were then used to automatically classify each scene using all available spectral bands and the respective models using the RStoolbox package (Leutner et al., 2019; R Core Team, 2018). The decision for a respective classification model was based on a visual inspection of the results and accuracy metrics.

To enable distance weighting (Broström et al., 2004; Calcote, 1995), plant abundances were estimated in fifteen 100 m wide concentric rings around each pollen sampling point (Figure 2a). The area of each land-cover class derived from the satellite data was then calculated for each ring using the packages rasterstats (Perry, 2013), pandas (McKinney, 2010), GDAL (GDAL/OGR contributors, 2012) and NumPy (Oliphant, 2006).

The woody vegetation cover for each ring (a) was transformed into taxa-specific cover (b) as follows. We first calculated the average abundance of selected woody taxa in the woody vegetation of each site (c) using field survey data. Second, we calculated the cover of selected woody taxa in each ring at each site (d; where d = a.c). Third, we calculated the abundance of each selected woody taxon in relation to the total cover of the selected woody taxa at each site (e). Finally we calculated the coverage of each selected woody taxon in each ring at each site (f; where f = d.e).

Modern pollen analysis

Pollen samples were prepared for pollen analysis following standard procedures (10% HCl, KOH, 40% HF – including 4 h boiling – and acetolysis; Faegri and Iversen, 1989; Moore et al., 1991). A minimum of 400 pollen grains were counted per sample using a microscope of ×400 magnification. Taxonomical identification was based on standard literature (Bonnefille and Riollet, 1980; Gosling et al., 2013; Leźine, 2005; Reille, 1995; Scott, 1982). Pollen percentages were calculated relative to the total terrestrial pollen sum.

We selected five pollen taxa according to their dominance in the regional vegetation and in the modern pollen spectra (Duffin

and Bunting, 2008): *Acacia* (incl. *Vachellia* sp. and *Senegalia* sp.), *Dichrostachys cinerea*, Combretaceae (incl. *Combretum* sp. and *Terminalia* sp.), *Grewia* (*Grewia* sp.) and Poaceae.

We estimated pollen fall speeds using Stoke's Law (Gregory, 1945), which predicts the settling velocity of spherical smooth particles smaller than 70 μm diameter. Although pollen grains have different structures and shapes, empirical studies have demonstrated that Stoke's Law is a reasonable theoretical predictor of pollen settling velocity (Borrell, 2012; Di-Giovanni et al., 1995; Gregory, 1973). In order to apply Stoke's Law to non-spherical pollen grains, we calculated the mean axis length for each taxon as the difference between the mean length of the major and minor axes (Mariani et al., 2016). Pollen size measurements were taken for at least 30 pollen grains of each selected taxon. Pollen grains were chosen at random from the slides of the surface samples from our study sites.

Pollen productivity estimates analysis

Pollen productivity estimates (PPEs) are calculated as pollen productivity ratios between two taxa (Broström et al., 2008; Bunting et al., 2013). In this study, we chose Combretaceae as the reference taxon (PPE = 1) because its pollen type is well represented in the pollen record and the corresponding species are common in the regional vegetation (i.e. *Combretum* sp. and *Terminalia* sp.). Furthermore, this approach allows for comparability of our results with a previous PPE study in African savannas by Duffin and Bunting (2008).

Although Poaceae is one of the main components of savanna vegetation, its use as a reference taxon in calibration studies is problematic because the pollen type is produced by many species which produce pollen in varying amounts and hence the resulting pollen signal can be highly variable (Baker et al., 2016; Li et al., 2015; Mariani et al., 2016). For comparison, we show a set of PPEs calculated with Poaceae as a reference taxon (Supplemental Table S1). We interpreted the taxa as low, medium or high pollen producers according to Kuneš et al. (2019).

For the calibration of pollen-vegetation relationships we use the ERV model, implemented as the ERVinR function in the R environment for statistical computing (Theuerkauf and Couwenberg, n.d.). This implementation follows the principles of the ERV sub-model 3 (Sugita, 1993, 1994). The latter builds upon the Prentice-Sugita model of pollen-plant abundance relationships (Prentice, 1985; Sugita, 1993):

$$y_{ik} = dwpa_{ik} * P_i + \omega_i \tag{1}$$

where,
y_{ik} = pollen loading of species i at site k (grains m^{-2})
$dwpa_{ik}$ = distance weighted plant abundance of species i at site k (m^2 m^{-2})
P_i = pollen productivity of species i per unit area (grains m^{-2})
ω_i = background pollen loading for species i (grains m^{-2})

Following this model, pollen loading of species i at site k is the sum of local pollen loading – calculated as distance-weighted abundances times pollen productivity – and background pollen loading. This model can be expressed in terms of percentage pollen values (ERV sub-model 3; Sugita, 1994):

$$pro_{ik} = \frac{dwpa_{iklocal} * P_i + \omega_{ikbackground}}{\sum^i dwpa_{klocal} * P + \omega_{kbackground}} \tag{2}$$

Under the assumption that the background pollen deposition of each taxon is similar at all sites, equation (2) can be used to approximate relative pollen productivity and background pollen deposition using a set of surface pollen and vegetation data (Sugita, 1994). The ERVinR function uses optimisation to find for each taxon those values of pollen productivity P and background

Table 2. Mean pollen grain size, fall speed estimates and calculated pollen productivity estimates (PPEs) for selected taxa. RegionCutOff was set to 10 km.

Taxa	Mean axis (μm)	Fall speed (m s^{-1})	PPE		PPE	
			GPM	SE	LSM	SE
Acacia	46.25	0.065	0.420	0.015	0.235	0.009
Dichrostachys	27.5	0.023	0.290	0.013	0.430	0.018
Grewia	47.13	0.067	0.230	0.010	0.090	0.004
Combretaceae	22.18	0.015	1.000	0.000	1.000	0.000
Poaceae	31.76	0.031	–	–	–	–

GPM: Gaussian plume model; LSM: Lagrangian stochastic model; SE: standard error. PPEs calculated with Poaceae as the reference taxon are presented in Supplemental Table S1.

pollen loading ω, with which percentage pollen values calculated with equation (2) are most similar to the observed pollen values. To this end, the ERVinR function uses conjugate-gradient optimisation from the 'optim' function from the {stats} package in *R*. The distance between pollen values modelled with equation (2) and the observed pollen values, which is minimized in the approach, is calculated as the mean squared chord distance. This distance is here used to evaluate the ERV application. Ideally, modelled and observed values are similar, that is they show a linear 1:1 relationship.

In ERVinR, the background pollen loading ω of each taxon is expressed as distance-weighted regional plant abundances multiplied by the respective pollen productivity. Rather than ω, ERVinR approximates the most suitable regional plant abundances of each taxon. This value can be compared to (if available) known regional plant abundances in the study area and hence is suitable for validation of the ERV application. Regional abundances of each taxon are assumed to be similar at all sites, so that the assumption of uniform background pollen loading holds.

To obtain the most reliable set of PPEs for this study, we proceeded as follows: first, we applied the ERVinR function comparing the GPM with the LSM as dispersal models for simulation of pollen flow for the five selected taxa. Second, we tested the ERV-model performance at three regional sizes (RegionCutOff) of 3, 10, and 50 km radius and repeated calculations 20 times to derive error estimates. Third, we repeated the analysis without Poaceae to identify the influence of this taxon on the model performance. Fourth, we selected the results obtained with the RegionCutOff and the number of taxa that yielded the best values and repeated calculations 100 times to derive PPE errors. The PPEs corresponding to the selected results were used in the REVEALS reconstruction. To assess the goodness of fit between the modelled pollen and the observed pollen percentages, we also calculated Pearson product-moment correlation analysis for each taxon.

Vegetation cover reconstruction

For the reconstruction of past vegetation cover we applied the REVEALS model (Sugita, 2007; Theuerkauf et al., 2016) to a fossil pollen record from Lake Otjikoto in Namibia (Tabares et al., 2020). The REVEALS model was applied using the GPM PPE values obtained in our study (Table 2). For Poaceae we used the PPEs calculated with Combretaceae as the reference taxon and available in the literature for savanna environments (PPE = 2.02; Duffin and Bunting, 2008). Due to the poor model fit obtained for Poaceae in our study (Supplemental Figures S4 and S5), we decided not to use the corresponding PPE value (Supplemental Table S3).

Model runs were performed using GPM, adjusted for neutral atmospheric conditions. Due to the lack of vegetation survey data
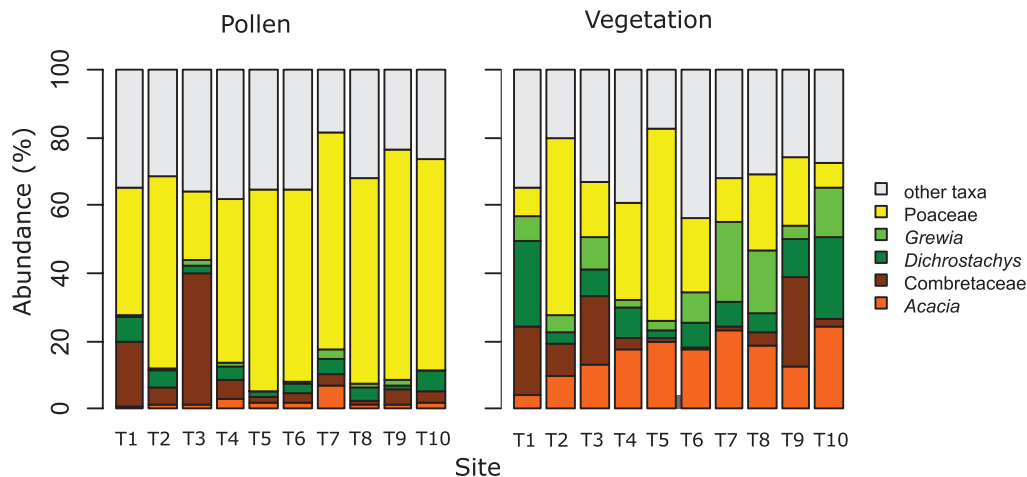
Figure 3. Pollen percentages and total vegetation abundances at the study sites.

from around the lake, we validated the REVEALS results against regional vegetation data obtained from satellite images. Since these were taken in the period 2012–2015, we calculated the mean cover estimates from the REVEALS results for the same period and compared them with the corresponding mean cover values obtained from satellite vegetation data from the northern Karstveld sites (T1–T5).

All analyses were performed in R software (R Core Team, 2018) with the package DISQOVER (http://disqover.botanik.uni-greifswald.de).

Results

Pollen assemblages and vegetation composition

We identified a total of 54 pollen types and 139 plant taxa (Supplemental Table S2). The total vegetation cover in the surveyed plots varies from 56% to 97%. The taxa selected for ERV analysis represented 56%–82% of the total vegetation cover (Figure 3). In the pollen record, the selected taxa represented between 62% and 81% of the total pollen sum.

Poaceae is the dominant pollen taxon at all sites, with the exception of T3, where Combretaceae pollen reaches high values (38%). Combretaceae also shows the greatest variation in the pollen (1.1%–38%) and vegetation data (0.7%–26%).

Acacia is rare in the pollen record (0.6%–6.7%) although more abundant in the vegetation (4.2%–24%). *Dichrostachys* and *Grewia* are also under-represented, reaching 25% and 23% in the vegetation but only 7.3% and 2.5% in the pollen record, respectively.

Pollen fall speeds and PPEs

Pollen fall speeds range between $0.014\,\mathrm{m\,s^{-1}}$ for Combretaceae as the smallest pollen type and $0.067\,\mathrm{m/s^{-1}}$ for *Grewia* as the largest pollen type (Table 2).

The resulting PPEs differ in response to the chosen dispersal model and the selected size of the region (RegionCutOff) (Supplemental Table S3). All calculations indicate higher pollen productivity in Combretaceae than in *Acacia, Dichrostachys* and *Grewia*. The PPE values of Poaceae (PPE range: 2.8–4.9) indicate the highest pollen productivity using both dispersal models (Supplemental Table S3A). Furthermore, we find that for the taxa with high pollen fall speeds – *Acacia* and *Grewia* – PPEs obtained with GPM are higher than PPEs obtained with LSM. For *Dichrostachys*, a taxon with a low pollen fall speed, PPEs obtained with GPM are lower than PPEs obtained with LSM.

Changing the size of the region (3, 10, or 50 km radius) has some influence on the resulting PPEs; they are mostly larger with a larger radius (Supplemental Table S3). Poaceae PPE

values are higher for LSM within a radius of 50 km compared to GPM. In addition, after excluding Poaceae from the calculations, PPE values increased and model performance improved (Supplemental Figure S4). Both dispersal models achieved the best fit at 10 and 50 km. We selected the results obtained in the 10 km radius for further calculations, because these showed smaller standard errors than for the 50 km radius (Supplemental Table S3). Final PPE and SE results (obtained after 100 iterations) are presented in Table 2.

Comparing the selected results from both dispersal models, the GPM has slightly lower optimisation scores than the LSM (Figure 4b). The standard errors of the PPE values are small for both models, however LSM results show lower SE values for *Acacia* and *Grewia* than GPM (Table 2). According to both models, *Grewia* is a low pollen producer (PPE <0.5). *Acacia* is a low to medium pollen producer (PPE: 0.4–1) according to the GPM, as is *Dichrostachys* according to the LSM.

Our results show high correspondence between modelled and observed pollen percentages for *Acacia* and Combretaceae and for both dispersal models (Figure 5). Observed and modelled pollen data match less well for *Grewia* and *Dichrostachys*. For *Grewia*, we see one clear outlier with high observed pollen values yet low modelled pollen values. The low modelled values reflect the low abundance of *Grewia* in the vegetation at site T9. We find no correspondence between observed and modelled pollen data for Poaceae (Supplemental Figure S5).

Vegetation reconstruction

The REVEALS model shows a mean Poaceae cover of 60% in zone 1 (Figure 6), which slightly increases in zone 2 (67%). Zone 3 is characterized by a sharp decrease of the Poaceae cover (mean cover 47%) and a corresponding increase in the cover of woody taxa (from zone 2 to zone 3: 32–52%). *Vachellia* and *Senegalia* (both corresponding to the *Acacia* pollen type) reach their highest cover values (*Vachellia*: 25%; *Senegalia*: 22%) in the 21st century.

Cover differences between regional vegetation and vegetation estimates are largest for *Acacia* and *Dichrostachys* (Figure 7a): the *Acacia* cover is overestimated (15%), while the opposite is observed for *Dichrostachys* (9.3%). Cover differences for the other taxa are smaller than 7.5%.

Discussion

PPEs and dispersal model

PPEs are a key parameter for reconstructing past landcover from pollen data. Following on from Duffin and Bunting (2008), we
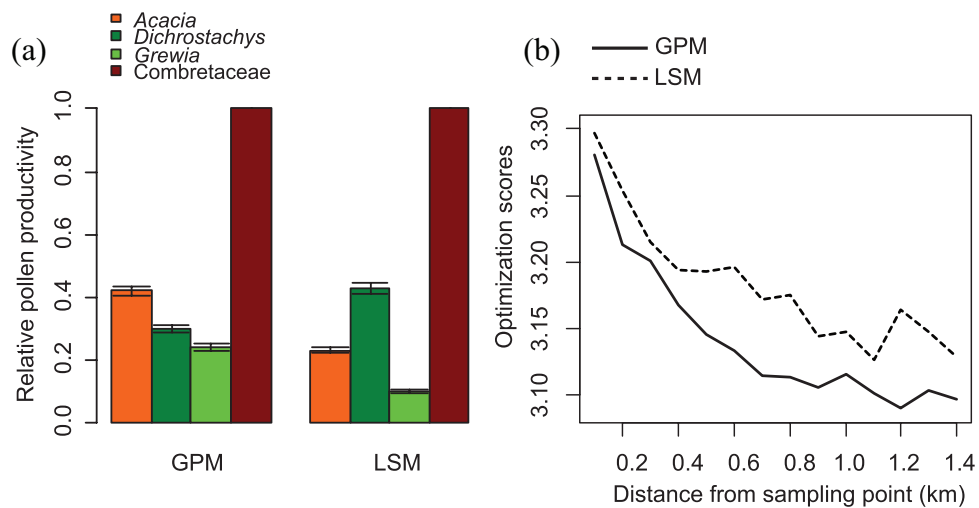
Figure 4. (a) Pollen productivity estimates (PPEs) with standard error. (b) Model performance obtained with the Gaussian plume model (GPM) and Lagrangian stochastic model (LSM) at 10 km radius without Poaceae.
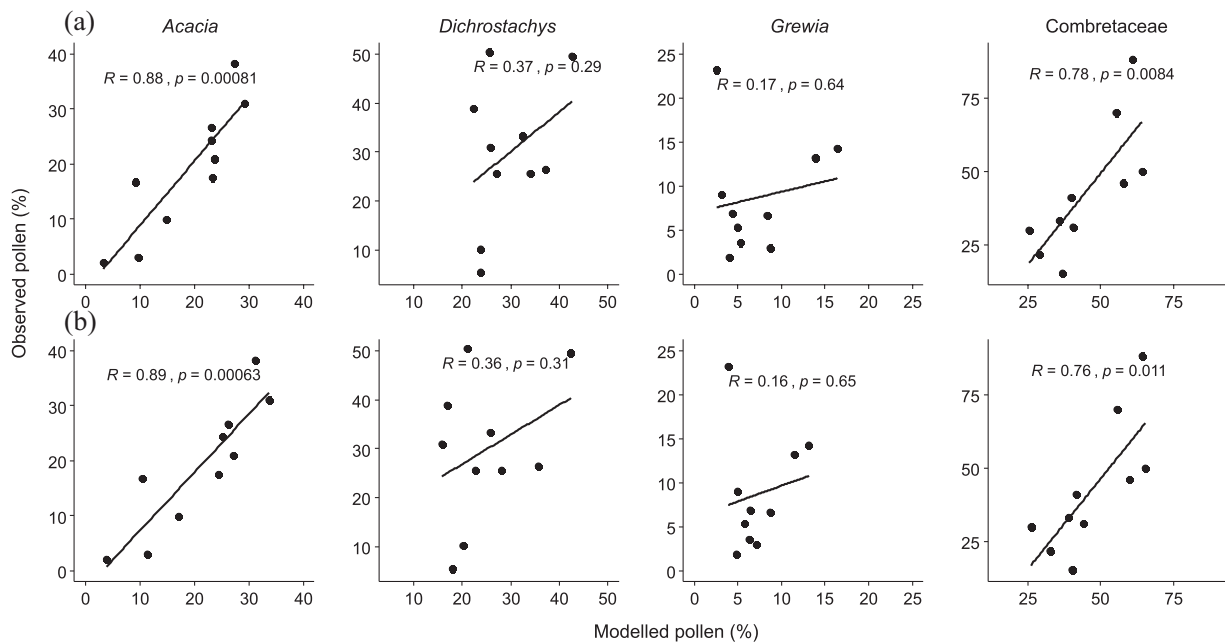

Figure 5. Pearson's correlation coefficient (*R*) and *p*-value (*p*) between observed and modelled pollen deposition (%) obtained with (a) Gaussian plume model (GPM) and (b) Lagrangian stochastic model (LSM) of dispersal at 10 km radius.
The results obtained by including Poaceae in the analysis are presented in Supplemental Figure S5.

here present the second study on PPEs for major savanna plant taxa of southern Africa. We present PPEs for *Grewia* and *Dichrostachys* for the first time, as well as PPEs for *Acacia* and Combretaceae using Poaceae as the reference taxon (Supplemental Table S1).

High pollen values and mostly much lower cover values of Poaceae (Figure 3) indicate that grasses are the highest pollen producers in the study region. However, our calculations failed to produce a close match between modelled and observed pollen values (Supplemental Figure S5), so uncertainty in the resulting PPE is high. There may be at least two reasons for this weak link between plant abundances and pollen deposition of grasses. First, the Poaceae pollen type is produced by many grass species, which probably differ in their pollen productivity (Prieto-Baena et al., 2003). So, the actual pollen deposition at each site is not only determined by the overall cover of grasses but also by the actual grass species composition at each site. Second, the cover and pollen production of grasses is much affected by grazing animals and

weather conditions, resulting in high seasonal and annual variations (de Morton et al., 2011; Groenman-van Waateringe, 1993; Tabares et al., 2018). The pollen in our top-soil samples likely originate from previous seasons as well as the current one, during which the cover of grasses may have been substantially different than during the time of our vegetation survey.

For the other taxa we find reasonably good correspondence between observed and modelled pollen data (Figure 5), indicating successful ERV application. Overall, the present study confirms the ranking of pollen productivity observed by Duffin and Bunting (2008), with decreasing productivity from Poaceae to Combretaceae and finally *Acacia* (Figure 4a). When calculated with GPM, as Duffin and Bunting (2008) did, we find that the PPE of *Acacia* is about half as high as that of Combretaceae.

Our comparison of PPEs produced with the two dispersal options have similar correlation coefficients for modelled and observed pollen values (Figure 5). With respect to regional vegetation composition, calculations with the LSM produce better
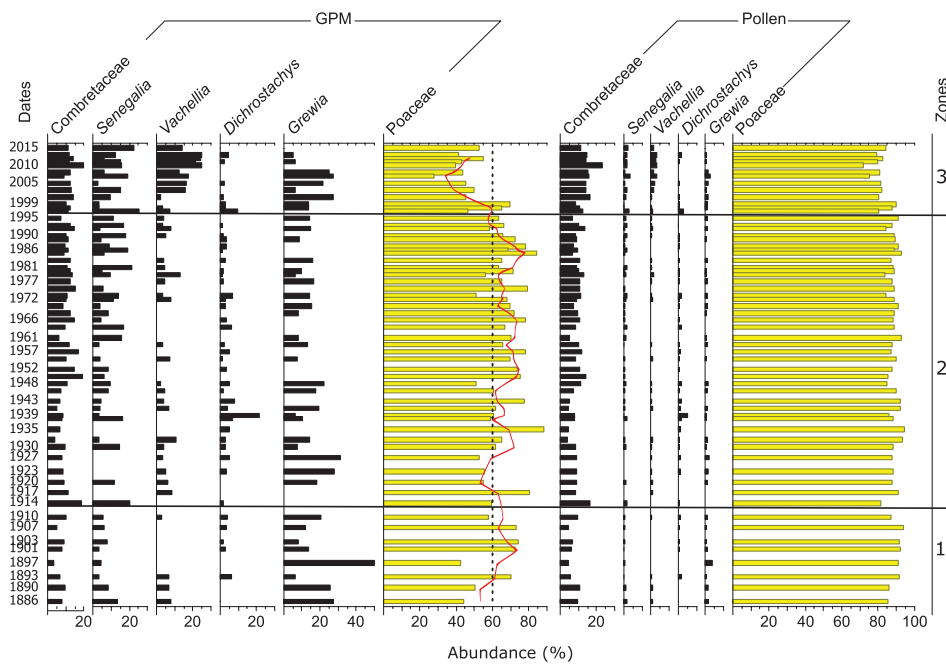
Figure 6. Quantitative vegetation reconstruction based on pollen data from Lake Otjikoto. REVEALS model using the Gaussian plume model (GPM) of dispersal (left). Original pollen percentages are also presented (right).
The red line denotes the grass cover running mean (calculated from three time points); the vertical black dotted line indicates the 50% grass cover. Pollen zones according to Tabares et al. (2020).
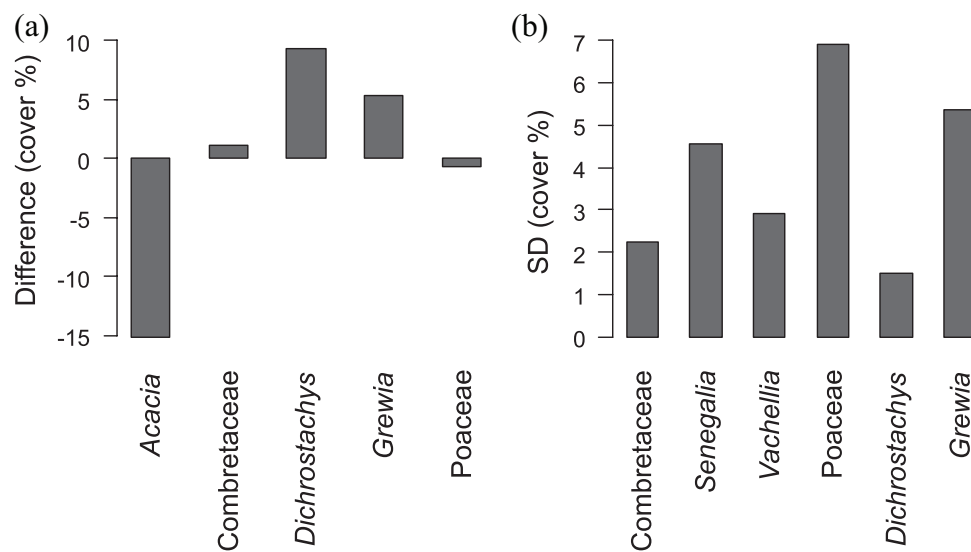

Figure 7. REVEALS statistics. (a) Cover differences between regional vegetation data and estimated abundances. (b) Average standard deviation (SD) from cover estimates of single taxa.

estimates for *Acacia* while calculations with the GPM produce better estimates for Combretaceae and Poaceae (Figure 7a). Hence, there is no clear indication that either dispersal option is more suitable. Still, the PPEs calculated with the LSM and GPM option differ substantially (Table 2). The effects are obviously related to the fall speed of pollen, which has a large influence in the GPM but not in the LSM (Kuparinen et al., 2007; Theuerkauf et al., 2013, 2016). Therefore, the GPM predicts much shorter dispersal distances for taxa with high fall speeds (*Acacia, Grewia*) than for taxa with low fall speeds (*Dichrostachys*). PPE calculations with the GPM thus tend to arrive at higher PPEs for taxa with high fall speeds to compensate for the lower predicted dispersal.

As mentioned above, our results do not clearly show whether the GPM PPEs or the LSM PPEs are more realistic. In general, calculations with the most realistic dispersal model will produce the most realistic PPEs. Limitations of the simple Gaussian plume model in describing dispersal particles are well known. Most notably, this class of models underestimates the contribution of pollen from distances greater than 10 km (Mariani et al., 2016; Theuerkauf et al., 2013). This is because the GPM is based on the existence of an isotropic field of winds and neutral atmospheric conditions (Pérez et al., 2018; Prentice, 1985), while the transport and contribution of pollen from distances greater than 10 km imply transient atmospheric states characteristic of unstable atmospheric conditions (Pérez et al., 2018).
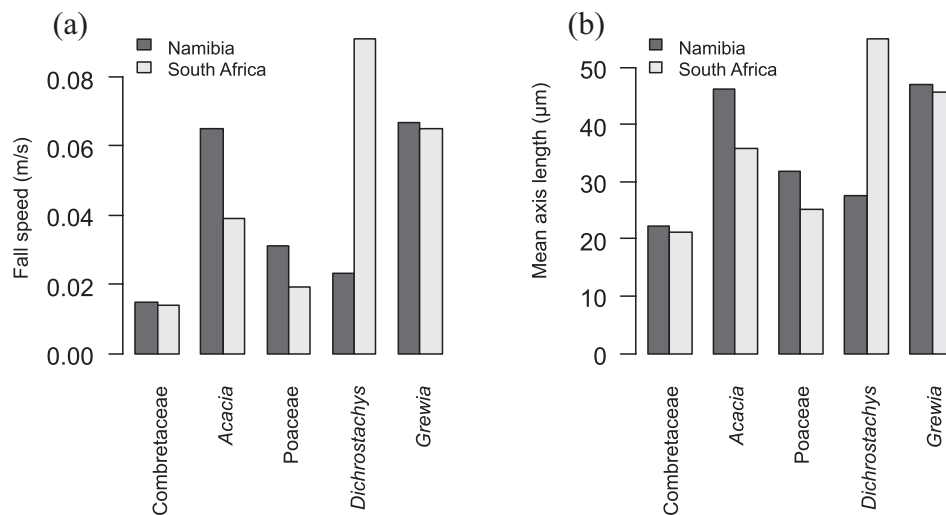
Figure 8. Pollen fall speed (a) and mean axis length (b) values of pollen grains from selected savanna taxa from Namibia (Table 2) and South Africa (Duffin and Bunting, 2008).

The far more complex Lagrangian stochastic dispersal models are much better suited to describe the contribution of long-distance pollen under unstable atmospheric conditions (Kuparinen et al., 2007), as well as the dispersal of pollen grains with high fall speeds (Kuneš et al., 2019). Hence, this class of models is state-of-the-art in all kinds of research related to atmospheric diffusion (Kuparinen, 2006; Lin et al., 2012). However, whether the general advantages of LSMs also apply to the present study is unknown. Both the GPM and the LSM dispersal option were applied using atmospheric parameters estimated for central and northern Europe. Whether these parameters are suitable for applications in tropical southern Africa still needs to be validated. For comparability with the study of Duffin and Bunting (2008), we have used the GPM option with parameters for neutral atmospheric conditions. However, unstable atmospheric conditions prevail during the day and in the summer months in southern Africa, while stable atmospheric conditions are dominant throughout the rest of the year (Luhunga and Mutayoba, 2013; Swart, 2017). Stable conditions inhibit vertical movement in the atmospheric boundary layer, resulting in low mixing height and low wind speed and consequently low dispersion and high concentration of airborne particles (Luhunga and Mutayoba, 2013; Stull, 1988; Swart, 2017). Under stable conditions, a low proportion of long-distance pollen can then be expected in the pollen record. We hypothesize that these conditions may partly explain the small source area of pollen observed for savanna species (Duffin and Bunting, 2008), as well as the local character of the pollen signal observed in Namibian savannas (Tabares et al., 2018). Also, and probably because of this, the GPM achieves a slightly better fit compared to the LSM (Figure 4b). Due to the importance of atmospheric conditions for the proper application of the dispersal model, we emphasize the need for further studies.

In the present study we have used pollen data from top-soil samples collected within semi-open vegetation. Pollen deposited at such sites not only arrives through atmospheric processes, but a significant amount of pollen may also arrive via flowering plants growing at the site, from soil material deposited by trampling animals or passing vehicles or via dung – all processes that are not represented in atmospheric dispersal models. Hence, even complex dispersal models may be of limited use to describe pollen deposition at such sites, and hence marginally suitable to calculate robust PPEs from such datasets. Future studies should therefore attempt to include pollen data from sites clearly dominated by atmospheric pollen deposition, such as from pollen traps in the absence of suitable lakes. Although the studied taxa are characterized by insect and animal pollination, pollen grains of *Acacia*,

Grewia, Combretaceae and *Dichrostachys* have usually been recorded in aerial pollen counts (Ezike et al., 2016; Julier et al., 2018; Kenrick, 2003; Zietsman, 1991).

Fall speed of pollen grains

We obtained pollen fall-speed values for *Grewia* and Combretaceae very similar to those calculated by Duffin and Bunting (2008) in South Africa (Figure 8a). However, the taxonomical composition of the pollen types likely constrains the regional applicability of fall-speed values. In our study, the pollen types of Poaceae and *Acacia* comprise different species with a wide range of sizes in pollen grains, such as *Aristida* sp. and *Heteropogon contortus* (L.) P. Beauv. ex Roem. & Schult. within the Poaceae type (mean axis range: 22–43 μm; Figure 8b), and *S. mellifera* and *Vachellia reficiens* (Wawra) Kyal. & Boatwr. within the *Acacia* type (mean axis range: 37–55 μm). This could explain the differences in the fall-speed values obtained by Duffin and Bunting (2008) for both taxa.

The discrepancy observed in the fall-speed values of *D. cinerea* between both studies probably results from methodological differences (i.e. it is not clear whether the cited authors measured single pollen monads or polyads, as they merged *D. cinerea, Albizia* sp. and *Acacia* sp. under the *Acacia* pollen type for ERV calculations). Differences in size measurements may also be related to variance in pollen preparation and sample storage.

Pollen size measurements may also depend on taphonomic processes, as we measured pollen grains taken from soil samples, while Duffin and Bunting (2008) measured pollen from lake sediments. Surface samples from lake sediments are commonly used for modern pollen analyses, while the use of surface soil samples has been questioned due to bias derived from poor pollen preservation (Han et al., 2017). However, pollen from surface soil samples are known to reflect the vegetation composition in savanna and arid environments well (Carrión, 2002; Tabares et al., 2018). In addition, the similarity between the mean axis values (Figure 8b) obtained for *Grewia* and Combretaceae and those obtained by Duffin and Bunting (2008) do not suggest shrinkage or deterioration of pollen grains in the two collection environments.

Quantitative vegetation reconstruction from around Lake Otjikoto

We quantified the change in landscape openness in a semi-arid savanna based on fossil pollen for the first time in southern Africa. The validation of our results with regional vegetation

data (Figure 7) confirms the suitability of REVEALS to be applied in savanna environments (Mariani et al., 2016). These results also help quantify past vegetation changes related to encroachment since the *Acacia*, Combretaceae and *Dichrostachys* pollen taxa comprise the main encroacher species in the Karstveld region (i.e. *S. mellifera, T. prunioides, D. cinerea*).

Application of REVEALS with the GPM model indicates a predominance of the semi-open landscape throughout the 20th century and a sharp decrease (~20%) in grass cover since 1990 linked to an increase in the cover of woody vegetation (Figure 6). The latter reflects the encroachment process in north-central Namibia and confirms previous studies (De Klerk, 2004; Tabares et al., 2020; Wessels et al., 2019).

Our results allowed us to quantify changes in the cover of grasses and woody taxa, which are associated with changes in land use and management during the last 130 years. In particular, the low percentages of grass cover in zone 1 may reflect broadscale fires related to field clearing as a management practice (Tabares et al., 2020), which is also suggested by the charcoal record (Supplemental Figure S6) and ancient DNA results obtained from a parallel sediment core from Lake Otjikoto (Tabares et al., 2020). Transhumance pastoralism and cropping took place in the vicinity of the lake at the turn of the 20th century. Interestingly, the low mean cover of tree taxa (~19% compared to 60% grass cover) may reflect the effect of combining fire and browsing, which has been assumed to prevent the establishment of tree seedlings (Gillson, 2004; Joubert et al., 2012). However, transhumance pastoralism may also have favoured the spread of *Grewia* through seed dispersal (Tews et al., 2004), which would explain its high abundance in zone 1.

During the first half of the twentieth century, changes in land tenure led to the construction of fences and the restriction of transhumance (Lau and Reiner, 1993; Mendelsohn et al., 2010). The concentration of livestock in turn led to changes in fire management, particularly the suppression of wildfires and/or the reduction of controlled fires to preserve pastures for livestock (Joubert et al., 2012). In addition, a rapid increase in livestock numbers up to the end of the 1950s followed the opening up of new grazing land (Lange et al., 1998), which is reflected by a 7% increase in the mean grass cover in zone 2. It is assumed that fire suppression affects grass/tree competition by reducing the mortality of seedlings and saplings (Case and Staver, 2017; Joubert et al., 2012), which would explain the spread of tree taxa (mean cover ~24%), particularly from the 1960s.

The decrease of grass cover since the 1990s, and particularly in the 21st century (average grass cover <50%), has been associated with overgrazing and prolonged droughts (Tabares et al., 2020). In particular, several studies have shown that high grazing pressure in pastures with low grass density reduces seed production and limits the potential of grasses to (re)invade niches (O'Connor and Pickett, 1992; Tessema et al., 2016). In addition, the effects of intensive grazing on the resilience of grasses are assumed to be greater under drought conditions (Souther et al., 2020).

A reduced grass cover in zone 3 (with lowest cover value of 27%) is related to an increase in woody cover (mean cover 52%), reflecting an encroached vegetation state. Such a change in the grass/woody ratio is also suggested by the pollen accumulation rates of woody taxa (Supplemental Figure S6), as well as by biogeochemical results (Tabares et al., 2020). Our findings support results from remote-sensing analyses, which have observed an increase in woody vegetation in north-central Namibia in the 21st century (Wessels et al., 2019).

The reduction of grass cover below 50% corresponds to a change from semi-open to thick savanna (Gil-Romera et al., 2010), while cover values below 30% reflect closed vegetation (Fisher et al., 2014). The grass cover estimates were also validated with regional vegetation data achieving cover differences of less than 7.5%, which suggests a close match with the vegetation data, as well as the accuracy of the Poaceae PPE (2.02; Duffin and Bunting, 2008) used in this study.

The spread of local encroachers *Vachellia* (likely *V. reficiens*), *Senegalia* (likely *S. mellifera*) and *Grewia* (likely *Grewia flava* DC.), demonstrate that changes in land openness in zone 3 correspond to changes in vegetation composition characteristic of an encroached vegetation state (Tabares et al., 2020). Cover estimates of woody taxa allow us to infer the magnitude of shrub encroachment in the region, although the interpretation of *Acacia* cover should be taken with care due to the overrepresentation of the estimated values.

Interestingly, such a change in woody vegetation cover can also affect local atmospheric conditions and pollen dispersal. Unlike temperate regions, where woody vegetation is expected to absorb more solar energy than grasses and thus increasing air convection (Baldocchi and Ma, 2013), studies conducted in semi-arid environments have shown that woody vegetation experiences lower surface temperatures than grassy areas due to effective convection heat loss and evaporative cooling (Rotenberg and Yakir, 2010). Therefore, the heat transfer to the atmospheric boundary layer decreases, as does the movement of convective air (Stull, 1988). Consequently, shrub encroachment can favour the prevalence of stable atmospheric conditions in the Namibian savannas, which can limit the long-distance contribution of pollen to the Lake Otjikoto record.

Conclusions

Our results extend the contribution of Duffin and Bunting (2008) and present new PPE values for *Grewia* and *Dichrostachys*, as well as PPE values for *Acacia* and Combretaceae using Poaceae as the reference taxon.

The ERV model failed to produce a close match with the observed pollen values for Poaceae. This is probably because this pollen taxon covers many species with different pollen productivities. Furthermore, grass productivity is affected by grazing and climatic conditions in savanna environments. ERV modelling was successful for the other taxa.

We also compared the PPEs produced with the GPM and LSM of dispersal. However, our results do not allow us to draw a conclusion on whether GPM PPEs or LSM PPEs are more realistic.

We considered at least two limitations with the dispersal models in our study. First, both the GPM and LSM dispersal options have been applied using atmospheric parameters estimated for central and northern Europe. Whether these parameters are suitable for applications in southern Africa needs to be validated. Furthermore, the deposition of pollen in soil samples, such as those collected in this study, occurs through processes that are not represented in atmospheric dispersal models. This suggests the need for pollen trap studies in the absence of suitable lakes in Namibia.

We also considered that the applicability of pollen fall speeds at a regional scale may be limited by the taxonomic composition of pollen types, as well as by differences in measurements resulting from methodology, pollen preparation and sample storage.

We obtained the first quantitative vegetation reconstruction for southern African savannas. Applying REVEALS to the pollen record of Lake Otjikoto allowed us to quantify changes in the cover of grasses and woody taxa associated with changes in land use and management during the last 130 years in north-central Namibia. Our results indicate a marked reduction in grass cover in the 21st century, as well as an increase in the cover of shrub species. Both changes reflect the encroachment trend observed by remote-sensing based studies in the region and seen in the vegetation composition. Validation of the REVEALS results with regional vegetation data confirms its suitability to be applied to fossil pollen records and to reconstruct vegetation history in savanna environments.

ORCID iD

Ximena Tabares [iD] https://orcid.org/0000-0002-9866-3843

Data availability statement

The data that support the findings of this study will be openly available in the PANGAEA repository

Supplemental material

Supplemental material for this article is available online.

References

Baker AG, Zimny M, Keczyński A et al. (2016) Pollen productivity estimates from old-growth forest strongly differ from those obtained in cultural landscapes: Evidence from the Białowieża National Park, Poland. *The Holocene* 26(1): 80–92.

Baldocchi D and Ma S (2013) How will land use affect air temperature in the surface boundary layer? Lessons learned from a comparative study on the energy balance of an oak savanna and annual grassland in California, USA. *Tellus B: Chemical and Physical Meteorology* 65(1): 19994.

Bonnefille R and Riollet G (1980) *Pollen Des Savanes d'Afrique Orientale*. Paris: Centre National de la Recherche Scientifique.

Borrell JS (2012) Rapid assessment protocol for pollen settling velocity: Implications for habitat fragmentation. *Bioscience Horizons* 5: hzs002–hzs002.

Braun-Blanquet J (1964) *Pflanzensoziologie. Pflanzensoziologie Grundzüge der Vegetationskunde*. Vienna: Springer.

Broström A, Sugita S and Gaillard M-J (2004) Pollen productivity estimates for the reconstruction of past vegetation cover in the cultural landscape of southern Sweden. *The Holocene* 14(3): 368–381.

Broström A, Nielsen AB, Gaillard M-J et al. (2008) Pollen productivity estimates of key European plant taxa for quantitative reconstruction of past vegetation: A review. *Vegetation History and Archaeobotany* 17(5): 461–478.

Bunting MJ, Farrell M, Broström A et al. (2013) Palynological perspectives on vegetation survey: A critical step for model-based reconstruction of Quaternary land cover. *Quaternary Science Reviews* 82: 41–55.

Calcote R (1995) Pollen source area and pollen productivity: Evidence from forest hollows. *The Journal of Ecology* 83(4): 591.

Carrión JS (2002) A taphonomic study of modern pollen assemblages from dung and surface sediments in arid environments of Spain. *Review of Palaeobotany and Palynology* 120(3–4): 217–232.

Case MF and Staver AC (2017) Fire prevents woody encroachment only at higher-than-historical frequencies in a South African savanna. *Journal of Applied Ecology* 54(3): 955–962.

De Klerk JN (2004) *Bush Encroachment in Namibia: Report on Phase 1 of the Bush Encroachment Research, Monitoring, and Management Project*. Windhoek: Ministry of Environment and Tourism, Directorate of Environmental Affairs.

de Morton J, Bye J, Pezza A et al. (2011) On the causes of variability in amounts of airborne grass pollen in Melbourne, Australia. *International Journal of Biometeorology* 55(4): 613–622.

Di-Giovanni F, Kevan PG and Nasr ME (1995) The variability in settling velocities of some pollen and spores. *Grana* 34(1): 39–44.

Duffin KI and Bunting MJ (2008) Relative pollen productivity and fall speed estimates for southern African savanna taxa. *Vegetation History and Archaeobotany* 17(5): 507–525.

Ezike DN, Nnamani C V., Ogundipe OT et al. (2016) Airborne pollen and fungal spores in Garki, Abuja (North-Central Nigeria). *Aerobiologia* 32(4): 697–707.

Faegri K and Iversen J (1989) *Textbook of Pollen Analysis*. 4th ed. Chichester: John Wiley & Sons.

Fisher JT, Erasmus BFN, Witkowski ETF et al. (2014) Savanna woody vegetation classification – Now in 3-D. *Applied Vegetation Science* 17(1): 172–184.

GDAL/OGR Contributors (2012) GDAL/OGR geospatial data abstraction software library. Available at: https://gdal.org (accessed 16 December 2020).

Gil-Romera G, Lamb HF, Turton D et al. (2010) Long-term resilience, bush encroachment patterns and local knowledge in a Northeast African savanna. *Global Environmental Change* 20(4): 612–626.

Gillson L (2004) Testing non-equilibrium theories in savannas: 1400 years of vegetation change in Tsavo National Park, Kenya. *Ecological Complexity* 1(4): 281–298.

Gosling WD, Miller CS and Livingstone DA (2013) Atlas of the tropical West African pollen flora. *Review of Palaeobotany and Palynology* 199: 1–135.

Gregory PH (1945) The dispersion of air-borne spores. *Transactions of the British Mycological Society* 28(1–2): 26–72.

Gregory PH (1973) *The Microbiology of the Atmosphere*. 2nd ed. London: L. Hill.

Groenman-van Waateringe W (1993) The effects of grazing on the pollen production of grasses. *Vegetation History and Archaeobotany* 2(3): 157–162.

Han Y, Liu H, Hao Q et al. (2017) More reliable pollen productivity estimates and relative source area of pollen in a forest-steppe ecotone with improved vegetation survey. *The Holocene* 27(10): 1567–1577.

Harris I, Jones PD, Osborn TJ et al. (2014) Updated high-resolution grids of monthly climatic observations – The CRU TS3.10 dataset. *International Journal of Climatology* 34(3): 623–642.

Hoffman MT, Rohde RF and Gillson L (2019) Rethinking catastrophe? Historical trajectories and modelled future vegetation change in southern Africa. *Anthropocene* 25: 100189.

Jackson ST and Lyford ME (1999) Pollen dispersal models in Quaternary plant ecology: Assumptions, parameters, and prescriptions. *The Botanical Review* 65(1): 39–75.

Joubert DF, Smit GN and Hoffman MT (2012) The role of fire in preventing transitions from a grass dominated state to a bush thickened state in arid savannas. *Journal of Arid Environments* 87: 1–7.

Julier ACM, Jardine PE, Adu-Bredu S et al. (2018) The modern pollen–vegetation relationships of a tropical forest–savannah

mosaic landscape, Ghana, West Africa. *Palynology* 42(3): 324–338.

Kenrick J (2003) Review of pollen–pistil interactions and their relevance to the reproductive biology of Acacia. *Australian Systematic Botany* 16(1): 119–130.

Kuneš P, Abraham V, Werchan B et al. (2019) Relative pollen productivity estimates for vegetation reconstruction in central-eastern Europe inferred at local and regional scales. *The Holocene* 29(11): 1708–1719.

Kuparinen A (2006) Mechanistic models for wind dispersal. *Trends in Plant Science* 11(6): 296–301.

Kuparinen A, Markkanen T, Riikonen H et al. (2007) Modeling air-mediated dispersal of spores, pollen and seeds in forested areas. *Ecological Modelling* 208(2–4): 177–188.

Lange GM, Barners JI and Motinga DJ (1998) Cattle numbers, biomass, productivity and land degradation in the commercial farming sector of Namibia, 1915–95. *Development Southern Africa* 15(4): 555–572.

Lau B and Reiner P (1993) *100 Years of Agricultural Development in Colonial Namibia: A Historical Overview of Visions and Experiments*. Windhoek: National Archives of Namibia.

Leutner B, Horning N and Schwalb-Willmann J (2019) RStoolbox: Tools for remote sensing data analysis. R Package Version 0.2.4. Available at: https://cran.r-project.org/web/packages/RStoolbox/ (accessed 16 December 2020).

Leżine AM (2005) African pollen database. Available at: http://apd.sedoo.fr/accueil.htm (accessed 26 March 2019).

Li Y, Nielsen AB, Zhao X et al. (2015) Pollen production estimates (PPEs) and fall speeds for major tree taxa and relevant source areas of pollen (RSAP) in Changbai Mountain, northeastern China. *Review of Palaeobotany and Palynology* 216: 92–100.

Lin J, Brunner D, Gerbig C et al. (eds.) (2012) *Lagrangian Modeling of the Atmosphere*. Washington, DC: American Geophysical Union.

Luhunga PM and Mutayoba E (2013) Variability of stability, momentum and heat fluxes in the stable boundary layer over highveld priority area, South Africa. *Applied Physics Research* 5(4): 23–36.

Mariani M, Connor SE, Theuerkauf M et al. (2016) Testing quantitative pollen dispersal models in animal-pollinated vegetation mosaics: An example from temperate Tasmania, Australia. *Quaternary Science Reviews* 154: 214–225.

McKinney W (2010) Data structures for statistical computing in Python. In: *Proceedings of the 9th Python in Science Conference*, 2010. Austin, TX: SciPy, pp.56–61.

Mendelsohn J, El Obeid S and Roberts C (2000) *A Profile of North-Central Namibia*. Windhoek: Gamsberg Macmillan.

Mendelsohn J, Jarvis A, Roberts C et al. (2010) *Atlas of Namibia. A Portrait of the Land and Its People*, 3rd edn. Cape Town: Sunbird Publishers.

Miller CS and Gosling WD (2014) Quaternary forest associations in lowland tropical West Africa. *Quaternary Science Reviews* 84: 7–25.

Moore P, Webb J and Collison M (1991) *Pollen Analysis*. Oxford: Wiley-Blackwell.

Neumann FH, Scott L, Bousman CB et al. (2010) A Holocene sequence of vegetation change at Lake Eteza, coastal KwaZulu-Natal, South Africa. *Review of Palaeobotany and Palynology* 162(1): 39–53.

O'Connor TG and Pickett GA (1992) The influence of grazing on seed production and seed banks of some African savanna grasslands. *The Journal of Applied Ecology* 29(1): 247–260.

Oliphant T (2006) *A Guide to NumPy*. USA: Trelgol Publishing.

Parsons RW and Prentice IC (1981) Statistical approaches to R-values and the pollen— vegetation relationship. *Review of Palaeobotany and Palynology* 32(2–3): 127–152.

Pérez CF, Bianchi MM, Gassmann MI et al. (2018) A case study of anisotropic airborne pollen transport in Northern Patagonia using a Lagrangian particle dispersion model. *Review of Palaeobotany and Palynology* 258: 215–222.

Perry M (2013) Rasterstats. Available at: https://github.com/perrygeo/python-rasterstats (accessed 16 December 2020).

Prentice IC (1985) Pollen representation, source area, and basin size: Toward a unified theory of pollen analysis. *Quaternary Research* 23(1): 76–86.

Prentice IC (1988) Records of vegetation in time and space: the principles of pollen analysis. In: *Vegetation History*. Dordrecht: Springer Netherlands, pp.17–42.

Prentice IC and Webb T (1986) Pollen percentages, tree abundances and the Fagerlind effect. *Journal of Quaternary Science* 1(1): 35–43.

Prieto-Baena JC, Hidalgo PJ, Domínguez E et al. (2003) Pollen production in the Poaceae family. *Grana* 42(3): 153–159.

R Core Team (2018) *R: A Language and Environment for Statistical Computing*. Vienna, Austria: R Foundation for Statistical Computing. Available at: https://www.r-project.org/ (accessed 16 December 2020).

Reille M (1995) *Pollen et Spores d'Europe et d'Afrique Du Nord*. Marseille: Laboratoire de Botanique Historique et Palynologie.

Rotenberg E and Yakir D (2010) Contribution of semi-arid forests to the climate system. *Science* 327(5964): 451–454.

Schüler L, Hemp A and Behling H (2014) Relationship between vegetation and modern pollen-rain along an elevational gradient on Kilimanjaro, Tanzania. *The Holocene* 24(6): 702–713.

Scott L (1982) Late Quaternary fossil pollen grains from the Transvaal, South Africa. *Review of Palaeobotany and Palynology* 36(3–4): 241–278.

Souther S, Loeser M, Crews TE et al. (2020) Drought exacerbates negative consequences of high-intensity cattle grazing in a semiarid grassland. *Ecological Applications* 30(3): e02048.

Stevens N, Erasmus BFN, Archibald S et al. (2016) Woody encroachment over 70 years in South African savannahs: overgrazing, global change or extinction aftershock? *Philosophical Transactions of the Royal Society of London. Series B, Biological sciences* 371(1703): 67–88.

Stull RB (1988) *An Introduction to Boundary Layer Meteorology*. Dordrecht: Kluwer Academic Publishers.

Sugita S (1993) A model of pollen source area for an entire lake surface. *Quaternary Research* 39(2): 239–244.

Sugita S (1994) Pollen representation of vegetation in quaternary sediments: Theory and method in patchy vegetation. *Journal of Ecology* 82(4): 881–897.

Sugita S (2007) Theory of quantitative reconstruction of vegetation I: Pollen from large sites REVEALS regional vegetation composition. *The Holocene* 17(2): 229–241.

Sutton OG (1947) The problem of diffusion in the lower atmosphere. *Quarterly Journal of the Royal Meteorological Society* 73(317–318): 257–281.

Swart A (2017) *Assessment of the Baseline Meteorological and Air Quality Conditions over Uubvlei Oranjemund Namibia*. Pretoria: University of Pretoria. Available at: http://hdl.handle.net/2263/60862 (accessed 16 December 2020).

Tabares X, Mapani B, Blaum N et al. (2018) Composition and diversity of vegetation and pollen spectra along gradients of grazing intensity and precipitation in southern Africa. *Review of Palaeobotany and Palynology* 253: 88–100.

Tabares X, Zimmermann H, Dietze E et al. (2020) Vegetation state changes in the course of shrub encroachment in an African savanna since about 1850 CE and their potential drivers. *Ecology and Evolution* 10(2): 962–979.

Tessema ZK, de Boer WF and Prins HHT (2016) Changes in grass plant populations and temporal soil seed bank dynamics in a semi-arid African savanna: Implications for restoration. *Journal of Environmental Management* 182: 166–175.

Tews J, Schurr F and Jeltsch F (2004) Seed dispersal by cattle may cause shrub encroachment of Grewia flava on southern Kalahari rangelands. *Applied Vegetation Science* 7(1): 89–102.

Theuerkauf M and Couwenberg J (n.d.) Pollen productivity estimates strongly depend on assumed pollen dispersal II: extending the ERV model. *The Holocene*.

Theuerkauf M, Couwenberg J, Kuparinen A et al. (2016) A matter of dispersal: REVEALSinR introduces state-of-the-art dispersal models to quantitative vegetation reconstruction. *Vegetation History and Archaeobotany* 25(6): 541–553.

Theuerkauf M, Kuparinen A and Joosten H (2013) Pollen productivity estimates strongly depend on assumed pollen dispersal. *The Holocene* 23(1): 14–24.

Wessels K, Mathieu R, Knox N et al. (2019) Mapping and monitoring fractional woody vegetation cover in the arid Savannas of Namibia using LiDAR training data, machine learning, and ALOS PALSAR data. *Remote Sensing* 11(22): 2633.

Zietsman PC (1991) Reproductive biology of *Grewia occidentalis* L. (Tiliaceae). *South African Journal of Botany* 57(6): 348–351.